Scripta METALLURGICA et MATERIALIA
Vol. 24, pp. 805-810, 1990
Printed in the U.S.A.
Pergamon Press plc

VIEWPOINT SET No. 14

WEAR-MECHANISM MAPS

M. F. Ashby* and S. C. Lim+,

*Engineering Department, Cambridge University, Cambridge CB2 1PZ, UK.
+National University of Singapore, Kent Ridge Road, Singapore 0511.

(Received August 15, 1989)
(Revised October 16, 1989)

WEAR-MECHANISM MAPPING: THE APPROACH

Wear is the loss or transfer of material when contacting surfaces slide. In general, the wear rate W (defined here as the volume loss per unit area of surface per unit distance slid) depends on the bearing pressure F/A_n (where F is the load carried by the contact and A_n is its nominal area), on the sliding velocity, v, and on the material properties and geometry of the surface (Figure 1):

$$W = f(F/A_n, v, \text{Mat. Props.}, \text{Geometry}) \quad (1)$$

But one such equation is not enough. There are many mechanisms of wear, each dependent in a different way on the variables. The dominant mechanism, at any given F and v, is the one leading to the fastest rate of wear. Table 1 lists some of the mechanisms encountered in wear studies of metals and of ceramics; it includes wear by melting, by chemical change induced by frictional heating, by low-temperature plasticity and by brittle fracture.

TABLE 1: MECHANISMS OF WEAR

METALS	CERAMICS
SEIZURE	SEIZURE (?)
MELT WEAR	MELT WEAR
SEVERE-OXIDATIONAL WEAR	THERMALLY-INDUCED STRUCTURE CHANGE
MILD-OXIDATIONAL WEAR	THERMAL CRACKING AND SPALLING
PLASTICITY-DOMINATED WEAR	BRITTLE SPALLING; INDENTION CRACKING
ULTRA MILD WEAR	TRIBOCHEMICAL WEAR

These mechanisms can be studied individually, and this, of course, is done. But it is also interesting to examine whether an overall framework can be found which reveals the relationships between the mechanisms, and identifies, for given sliding conditions, the one likely to be dominant. Two converging routes are available.

The first is empirical. Data from wear experiments are plotted on suitable axes (F/A_n and v, for example) and identified by wear rate and mechanism. Boundaries are drawn to separate classes of behaviour, separating all data points associated with one mechanism from those associated with another. The result (shown for the dry sliding of a medium-carbon steel on itself in Figure 2) identifies the field of dominance of each mechanism. It is like classifying animals by counting the number of legs, observing whether they have horns, are furry, and so on.

0036-9748/90 $3.00 + .00

The second route is that of physical modelling. The individual mechanisms of wear (Table 1) are identified. A wear-rate equation with the form of equation (1), based on microscopic modelling (using the principles of mechanics, thermodynamics, chemical kinetics and so forth) is derived for each mechanism. The dominant mechanism is identified with the mechanism which, at a given F and v, gives the fastest wear rate. A diagram like Figure 2 - but based on physical reasoning, not merely on observation - can then be constructed from the models. It is more like classifying animals by examining their genetic code.

The two approaches are complementary. Each mechanism of wear is complicated - too complicated to hope that a physical model can be constructed from first principles which will describe it with useful precision. The model identifies the important variables and their functional relationship: power law, exponential, logarithmic, and so on; but, to be useful, each model must be calibrated. The empirical approach identifies blocks of data which characterise a given mechanism. A block is used to calibrate the appropriate equation. The calibrated equations are used to construct the maps.

The result of applying this combined procedure is shown for steel-on-steel in Figure 3. The axes, as before, are F/A_n and v. Heavy lines identify field boundaries, separating fields in which a single mechanism is dominant. The equations themselves (each with the form of equation (1)) describe the wear-rate, W. It is shown on the figure as a set of contours of constant W. The figure summarises an enormous amount of information (both that contained in the models and that in the data) and provides an overview of the wear behaviour of a given sliding pair over a wide range of sliding conditions.

The method (1) is still in its infancy. The rest of this article gives further details, indicating the degree to which progress has been made with aspects of modelling, and where further work is needed.

THE TEMPERATURES AT A SLIDING SURFACE

When contacting solids slide, almost all the work done against friction appears as heat. The heat is partitioned between the two solids, raising their temperatures. The local increase in temperature influences the rate of wear and (together with the other variables of equation (1)) determines the dominant wear-mechanism.

Two temperatures are of interest: the "bulk" or average temperature, T_b, of the near-contact region, and the "flash" or local temperature peaks, T_f, at the asperities on the surface where true contact is actually made. In calculating these (by standard heat-flow methods) allowance must be made for both steady-state and transient heat flow, for the differing thermal properties and geometry of the two solids which meet at the surface, and for the thermal contact-resistance between these and the clamps to which they are attached. This has been done for a number of standard test geometries (pin-on-disk, flat-on-flat, ball-on-plate and so forth). The results (2) are best presented as temperature maps of which Figure 4 is an example. It shows, on the same axes as before (F/A_n and v) the bulk and flash temperatures which appear when a low-carbon-steel pin slides on a disk of the same material. The lowest contour of each group corresponds to the onset of heating: at lower values of F and v, the frictional heat is quickly conducted away and the surfaces remain cold; here mechanisms of "cold" wear will dominate. The uppermost contour of each group corresponds to the melting temperature of the steel: above the upper contour for the bulk temperature, general melting occurs; here wear is very rapid. Below, but above the lowest contour, there is substantial heating; here heat-induced mechanisms involving oxidation, chemical reaction and thermal softening and shock will dominate. These temperature-maps, which have been explored for a number of metal and ceramic sliding couples (Ashby et al, (2)), are the starting point for constructing model-based wear mechanism maps.

WEAR MECHANISMS

The modelling of wear mechanisms is reviewed elsewhere (1). Briefly, the background is as follows.

When the normal pressure on the interface is very large, any attempt to induce sliding causes the real contact area A_r (the area of contact of the asperities at which the two surfaces touch) to grow until it becomes equal to their nominal area, A_n, and the surfaces seize. This determines the position of the uppermost almost horizontal, boundary on Figure 3: the seizure line. Seizure is the goal when parts are joined by "wringing" them together.

When the bulk temperature T_b exceeds the melting temperature T_m, the lower-melting surface is ablated rapidly by melt wear, involving the ejection of liquid droplets or sparks, a phenomenon made use of in frictional cutting and welding. The position of the melt wear field in Figure 2 is derived directly from the temperature map, Figure 4. (Flash temperatures which exceed melting do not cause this sort of melt wear because the molten asperity-tip flows over cooler, adjacent material and resolidifies.) Melt-wear occurs beneath skis and skates, leaving ruts on much-travelled paths.

Conditions not severe enough to produce melting can still cause severe oxidation, and thermal-induced property changes which we will refer to as severe-oxidation wear. The conditions are such as to produce high temperatures in the near-surface region; the resulting chemical reactions give a brittle surface layer (an oxide, for example), which spalls off. The wear rate is determined by the temperature (hence the importance of Figure 4) and the kinetics of the chemical change; modelling of the wear rate starts from a kinetic model for the reaction. A steel cutting tool such as a twist drill, run under severe conditions, shows this sort of chemical attack.

At still lower sliding velocities and bearing pressures the frictional heat is conducted away from the sliding surfaces which no longer suffer general heating. But at the small areas of true contact where all the heat is generated (Figure 1), high flash temperatures still appear (Figure 4). Although the bulk of the surface is cold, the asperity tips are hot enough to oxidise; the oxide is scraped off by the sliding action, and other classes of mechanism - that of mild-oxidational wear in metals, and perhaps thermal-shock wear in ceramics - take over. Modelling again requires combining a calculation of the local temperature with a kinetic model for the oxidation process. It leads to the field labelled "mild-oxidational wear" on Figure 3. The mechanism is an important one, dominant for many metals in the regime of low bearing pressure and sliding velocities around 1 m/s - a common range in machine tools, engines, motors, etc.

At sliding velocities below about 0.1 m/s for metals (but nearer 0.01 m/s for ceramics and polymers) there is no significant heating of any sort. Wear, here, is by "cold" mechanisms. In a non-aggressive environment - one in which no corrosive attack takes place - wear of ductile materials is dominated by plasticity-dominated mechanisms": fragments are removed by transfer from one surface to the other, or by sub-surface cracking. Wear of brittle materials, under similar conditions, is by brittle fracture and edge-spalling. Despite their wide occurrence (they are the primary mechanism of low-speed wear) and the considerable effort which has been expended in studying them, they are insufficiently understood to model well. Both, empirically, are approximately described by Archard's law

$$W = K_a F \qquad (2)$$

where K_a is a constant.

Under extremely mild conditions (very low F/A_n and v) even the contribution of plasticity becomes negligible. In the ultra-mild wear regime it is thought that the surfaces skate over each other without breakdown of the adsorbed gas layer, or very

thin oxide film, which forms even at room temperature. For metals, the wear debris is found to be an oxide (not metallic, as it is in plasticity-dominated wear), and the wear rate is low; but these very mild conditions are rarely encountered in practice. Corrosion, of course, changes everything by creating a corrosion product, which may be easily removed by sliding, leading to rapid wear again.

The wear-rate equations differ in the soundness of their physical base. Seizure and melt-wear can be modelled from first principles, with no adjustable parameters. The physics of thermally-induced oxidation and chemical change is well understood, but the modelling involves kinetic constants which are not known from first principles with the precision we require; the equations for these mechanisms must be calibrated to experiment. The models for the cold mechanisms are yet more difficult: the physical basis of the modelling guides the form of the equation and ensures that it contains the right material properties, but calibration to experiment is essential here also. The empirical plot (Figure 2) helps here. It identifies blocks of data which can be associated with a given mechanisms. A subset of this block is used to calibrate (i.e. to set the uncertain constants, coefficients or exponents) in the model-based equations; the rest is used to check that the model now describes the mechanism well.

THE CONSTRUCTION OF WEAR-MECHANISM MAPS

The picture so far: wear involves many competing mechanisms, one set for ductile materials like metals, a different set for brittle ceramics, with some overlap; each mechanism can be modelled, with varying degrees of precision, to give a set of equations with the form of equation (1); each such equation can be calibrated against experiment, thereby establishing the uncertain constants or coefficients it contains, and checked by examining how well the calibrated equation describes the remaining data or new measurements. We now wish to present this information in a clear and useful way.

There is no universal wear diagram, because the controlling variables differ from mechanism to mechanism. But the plot used here, with F/A_n and v as axes, is a good first choice, for two reasons: first, because these two variables directly determine surface temperature and, through this, the rates of "hot" mechanisms and the upper boundary of the "cold" ones; and, second, because they are variables which are under the control of the operator, and are easily measured. The wear-map (Figure 3) is constructed by identifying the dominant mechanism with that which, in a given field of F/A_n and v, gives a higher wear rate W than does any other mechanism. The field boundaries are lines along which two mechanisms give the same wear-rate; they are found by equating the wear-rate equations, taken in pairs. The contours show the total wear rate W; it is the sum of the contributions from all the mechanisms. Reality is, of course, more complex: mechanisms may interact in a damaging way; wear can be caused by foreign bodies (grit; combustion products) and by environmental attack (corrosion, water-induced slow crack growth) and there are all the effects of lubrication. It must be emphasised that their absence from the diagrams shown here is not a deficiency of the method. They could, in principle, be included; they are omitted at this stage to keep the number of independent variables - the number of dimensions of the problem, so to speak - within bounds.

The result of all this is a diagram like Figure 3. It contains information from, and thus summarises, the thermal calculations, the wear-rate models, and the experimental data used to calibrate them all. It identifies the field of dominance of each mechanism, shows the relationship between mechanisms, and indicates where wear-rate transitions (3) take place. The method reveals that some models cannot adequately explain the data, and thus highlights deficiencies in our understanding of mechanisms, where further work is needed.

How successful is the method? In the "hot" regimes the dominant factor is the surface temperature, and this is directly dependent on F/A_n and v. Here evidence suggests that the method works well. In the "cold" regime, the sliding velocity v

ceases to be an important variable (it does not appear in Archard's equation, equation (2)); other, less easily-controlled variables do matter, the surface roughness and the surface shear strength (which measures the strength of adhesion across the surface). For like surfaces (steel-on-steel, for instance) it can be argued that the surface "conditions" itself; that is, after a running-in period, the evolved surface roughness depends only on F/A_n and v, not on initial roughness; but for unlike surfaces this is certainly not so. Then a new set of axes is needed to describe wear in the cold regimes. Work is in progress on this and other aspects of the problem.

CONCLUSIONS AND FUTURE DEVELOPMENTS

Considered in the broadest context, wear involves many mechanisms. Most studies, quite properly, focus on the narrow range of sliding conditions and the single mechanism associated with a given application. But it is also helpful, sometimes, to step back and try to get a view of the whole picture. That is the motivation for the mechanism-mapping approach developed here. The approach combines physical modelling with experimental data.

There is no universal projection for this map. One useful one is that of using the sliding conditions, F/A_n and v, as axes, since they are controllable and determine many aspects of wear behaviour, among these, surface heating. On these axes, the fields of dominance of each mechanism can be shown, and the wear rate itself plotted as a set of contours.

Doing this for metallic systems reveals a number of mechanisms: melt wear, "hot" mechanisms involving oxidation, phase change or chemical reaction, and "cold" mechanisms dependent on material transfer by plasticity and crack growth. For these materials, the choice of axes works well for the hot mechanism, but is less good for the cold ones in which surface roughness, R, and adhesion play an important part: an "inset" using a different set of axes (F/A_n and R, for instance) may be more appropriate here. The wear of sliding couples which involve ceramics and polymers is less well understood, but is also known to involve many mechanisms. The mapping technique is currently being applied to these also.

As a step in this direction software is under development to allow surface temperature to be computed for any sliding couple, in any one of a number of common geometries. This will form the basis of a more elaborate programme to construct wear-mechanism maps for a range of commonly studied materials. In the longer term, there is the possibility of including lubrication in the treatment, allowing description of a much wider range of bearing systems.

ACKNOWLEDGEMENTS

The authors wish to acknowledge the support of the US DOE-ECUT Tribology Program through Contract Number (RFP) 88-47DH-D35 with Argonne National Laboratories.

REFERENCES

The methodology described here draws on a body of published work far too large to cite adequately in the restricted length of this short report. The papers below deal directly with wear-mapping, and contain references to the wider literature.

(1) S. C. Lim and M. F. Ashby, Acta Metall 35, 1, (1987).

(2) M. F. Ashby, J. Abulawi and H-S Kong. Cambridge University Engineering Department Report CUED TR/MATS 89 (1989).

(3) S. C. Lim, M. F. Ashby and J. H. Brunton, Acta Metall 35, 1343, (1987).

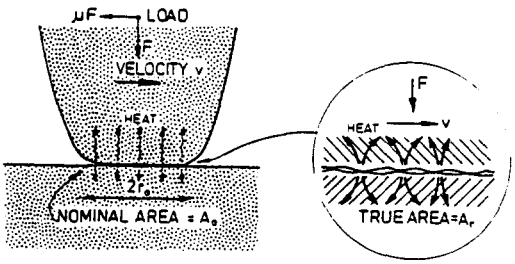

Figure 1. A typical sliding couple. The nominal contact area is A_n, but the true area of contact, A_r, is usually much smaller.

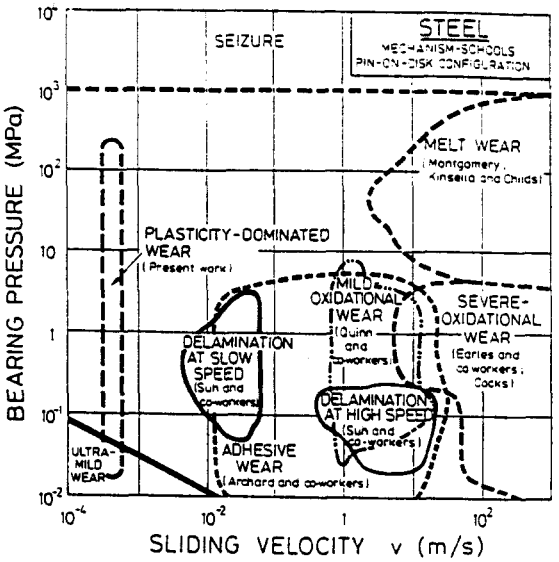

Figure 2. An empirical map of wear mechanisms, constructed by drawing boundaries around fields in which a given mechanism is observed, a medium-carbon steel sliding on itself.

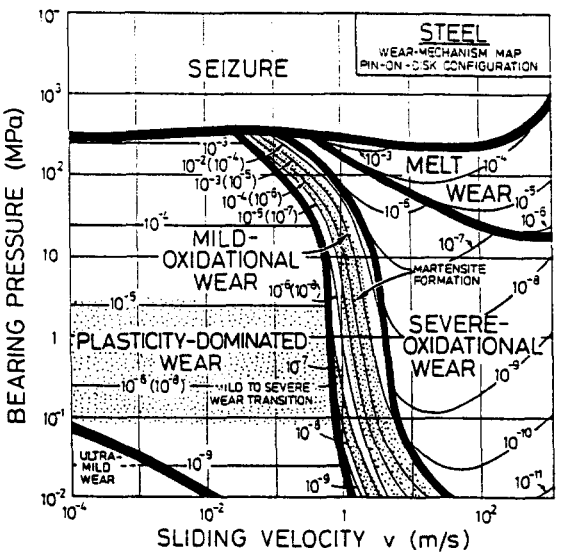

Figure 3. A wear-mechanism map for low-carbon steel based on physical modelling calibrated to experiments. The shaded regions show transitions.

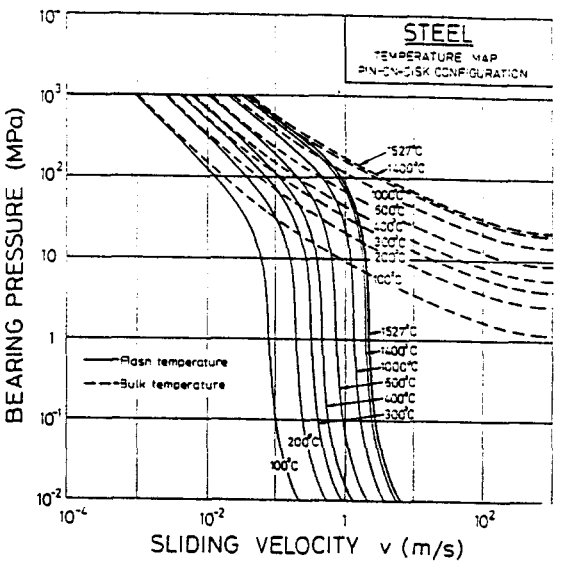

Figure 4. A temperature map for a low-carbon steel pin sliding on a steel disk. Bulk temperature contours are shown as broken lines, flash temperatures as full lines.